

# ChemComm

Accepted Manuscript



This is an *Accepted Manuscript*, which has been through the Royal Society of Chemistry peer review process and has been accepted for publication.

*Accepted Manuscripts* are published online shortly after acceptance, before technical editing, formatting and proof reading. Using this free service, authors can make their results available to the community, in citable form, before we publish the edited article. We will replace this *Accepted Manuscript* with the edited and formatted *Advance Article* as soon as it is available.

You can find more information about *Accepted Manuscripts* in the [Information for Authors](#).

Please note that technical editing may introduce minor changes to the text and/or graphics, which may alter content. The journal's standard [Terms & Conditions](#) and the [Ethical guidelines](#) still apply. In no event shall the Royal Society of Chemistry be held responsible for any errors or omissions in this *Accepted Manuscript* or any consequences arising from the use of any information it contains.



## Hollow Tubular Porous Covalent Organic Framework (COF) Nanostructures

Received 00th January 20xx,  
Accepted 00th January 20xx

Pradip Pachfule,<sup>a</sup> Sharath Kandmabeth,<sup>a,b</sup> Arijit Mallick,<sup>a,b</sup> Rahul Banerjee<sup>a,b\*</sup>

DOI: 10.1039/x0xx00000x

www.rsc.org/

**The hollow and tubular TpPa-COF structures have been synthesized by template-assisted replication of nanometer sized ZnO-nanorods. The hollow structures composed of microporous TpPa shell have high periodicity, moderate porosity, chemical stability and capsule shaped morphology as revealed from X-ray diffraction, porosity measurements, SEM and TEM analyses.**

The synthesis of micron and nanometer sized low density hollow structures have received considerable attention in recent years.<sup>1</sup> These hollow structures have been successfully utilized for their applications in drug delivery, catalysis, sensing and confined-space chemical reactions, etc.<sup>2</sup> Although self templated synthesis of hollow structures have been attempted to some extent, the synthesis of hollow structures by templating strategies provide significant advantages in size and shape control as well as freedom of template variability.<sup>3</sup>

In recent years, hollow nanostructures composed of porous and crystalline materials such as zeolites, metal oxides and metal organic frameworks (MOFs) have been synthesized by molding these materials on various removable organic/inorganic templates.<sup>4</sup> However, the toxic nature of such hollow materials arising from constituting metals and other hazardous components with very limited stability in aqueous, acidic and basic mediums restricts their usages for specific bio-compatible applications such as drug storage, drug delivery, tissue-engineering, etc.<sup>5</sup> Hence, bio-compatible materials synthesized from purely organic substituents and high chemical as well as thermal stability are desired for such applications. Although the synthesis of hollow structures composed of purely organic materials *viz.* polyanhydrides and conjugated microporous polymers have been attempted, their limited chemical stability in aqueous, acidic and basic mediums and amorphous

nature brings limitations to their applications.<sup>6</sup> In this regard, crystalline covalent organic frameworks (COFs) may be useful for constructing such hollow structures.<sup>7</sup> Recently, we and others have explored the synthesis of porous and crystalline COFs with exceptional chemical stability.<sup>8</sup> Since these COF crystallites have internal defects, the long-range growth or construction of COF hollow structures using these chemically stable COFs has not been explored much.<sup>9</sup> Herein, we for the first time, report the synthesis of chemically stable hollow **TpPa** COF<sup>10</sup> nanostructures with capsule shaped morphology *via* template assisted synthesis (Fig. 1a).

The hollow structures of **TpPa** COF have been synthesized through template-assisted replication of nanometer sized ZnO-nanorods (Fig. 1b). The synthesis of hollow **TpPa** nanostructures was carried out in two steps. In the first step the synthesis of hybrid structures with ZnO-nanorods as a core and **TpPa** COF as a shell (**ZnO@TpPa**) has been performed by the reaction of 1,3,5-triformylphloroglucinol (**Tp**) with *p*-phenylenediamine (**Pa**) in 1:1 mesitylene/dioxane solvent in presence of pre-synthesized and well dispersed ZnO-nanorods (Fig. 1a), using acetic acid in catalytic amount (3 M, 50  $\mu$ L).<sup>10</sup> In the second step these hybrid structures were subjected to the acid treatment (1N HCl) for 24 h to achieve the selective and complete removal of the ZnO-nanorods and to obtain the hollow **TpPa** nanostructures in quantitative yield. The PXRD profile of **ZnO@TpPa** matches well with corresponding peaks of simulated XRD patterns of **TpPa** COF (eclipsed stacking model)<sup>10</sup> and ZnO-nanorods (JCPDS 89-1397)<sup>11</sup> indicating the self-assembly of both materials (Fig. 1c; Section S7, ESI). The broad peaks at 4.7° (100 plane), 8.3°, 11.1° and 27° (001 plane) corresponds to **TpPa** COF; whereas the sharp peaks at 32.2°, 34.8° and 36.7° represent the presence of ZnO in nano-form. The selective and complete removal of ZnO-nanorod from **ZnO@TpPa** was confirmed by PXRD analysis (Section S4 and S5, ESI). The well maintained PXRD patterns of hollow **TpPa** with intact peaks for (100) and (001) planes appearing  $\sim 4.7^\circ(2\theta)$  and  $\sim 27^\circ(2\theta)$  demonstrated the selective removal of the ZnO-nanorods with retention of **TpPa** COF hollow structure integrity and minimal loss of crystallinity (Fig. 1c).<sup>12</sup>

The FT-IR spectra of **ZnO@TpPa** indicate the presence of all the characteristic peaks of **TpPa** verifying the formation of **TpPa** COF on the surface of ZnO-nanorods (Fig. 1d). Similar FT-IR spectrum

<sup>a</sup>Physical and Materials Chemistry Division, CSIR-National Chemical Laboratory, Dr. Homi Bhabha Road, Pune 411008, India.

<sup>b</sup>Academy of Scientific and Innovative Research (AcSIR), New Delhi 110 025, India.  
E-mail: r.banerjee@ncl.res.in; Tel: +912025903205

† Electronic Supplementary Information (ESI) available: Detailed experimental procedures, PXRD plots, SEM and TEM images, EDAX analyses, adsorption analyses details and additional supporting data. See DOI: 10.1039/x0xx00000x

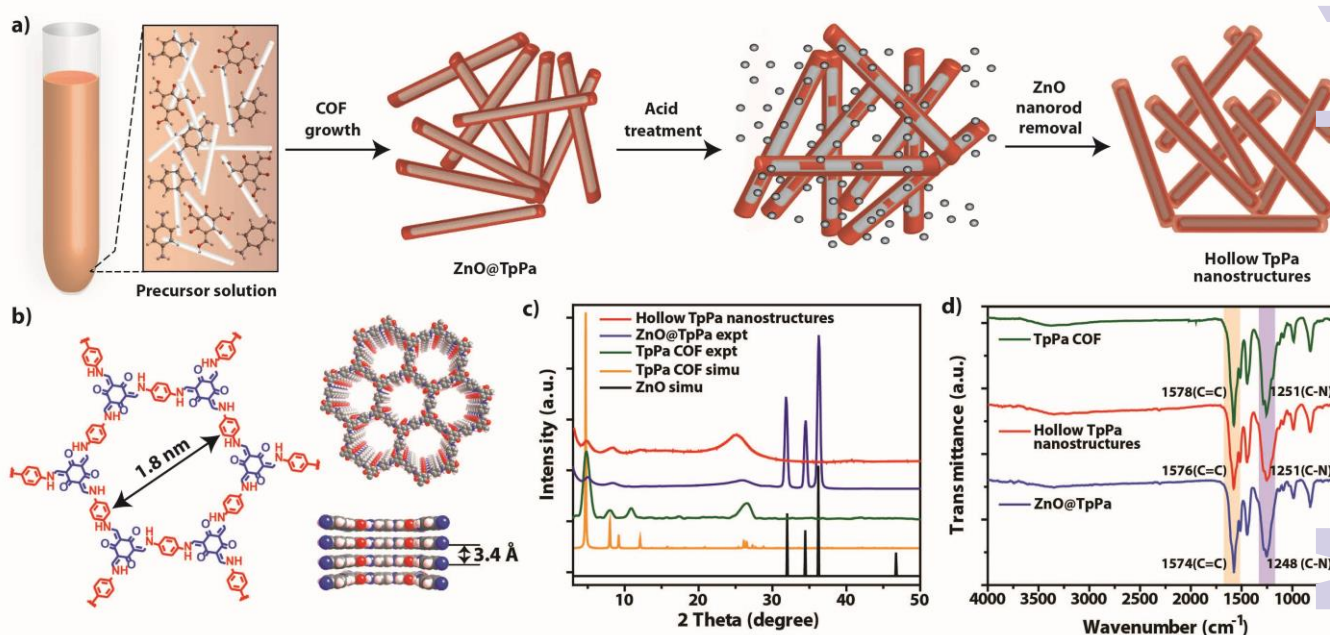


**Fig. 1** Synthesis and characterization of COF nanostructures. (a) Scheme of synthesis of highly stable and hollow COF structures *via* templating strategy by *in situ* solvothermal reaction of 1,3,5-triformylphloroglucinol (**Tp**) and *p*-phenylenediamine (**Pa**), in presence of ZnO-nanorods in mesitylene-dioxane solvent. (b) The structure and packing diagram of **TpPa** COF showing microporous architecture. (c) Comparison of the experimental PXR patterns of hollow **TpPa** nanostructures, **ZnO@TpPa** and pristine **TpPa** COF with simulated PXR patterns of **TpPa**-COF and ZnO-nanorods (JCPDS 89-1397). (d) Comparison of the FT-IR spectra of hollow **TpPa** nanostructures, **ZnO@TpPa** with the pristine **TpPa** COF.

observed for hollow **TpPa** nanostructures confirmed that even after strong treatment with 1N HCl for 24 h, the chemical composition of the COF framework remained intact (Fig. 1d). The appearance of strong representative peaks for C=C ( $\sim 1578\text{ cm}^{-1}$ ) and C-N ( $\sim 1251\text{ cm}^{-1}$ ) stretching for **TpPa** in **ZnO@TpPa** and hollow **TpPa** confirmed the formation of COF on top of ZnO-nanorods and selective removal of ZnO from hybrid **ZnO@TpPa** without disturbing the basic **TpPa** architecture. The formation of imine bond and the existence of **TpPa** COF in the enol form was further confirmed from the  $^{13}\text{C}$  CP-MAS solid-state NMR spectrum (Fig. 2a). These  $^{13}\text{C}$  CP-MAS data showed the similar location of the imine carbon peaks ( $\sim 145\text{ ppm}$ ) and carbonyl carbons peaks ( $\sim 183\text{ ppm}$ ) of the **TpPa** COF and **ZnO@TpPa**, which indubitably confirms the formation of COF on the surface of ZnO-nanorods. The matching  $^{13}\text{C}$  CP-MAS spectrum for hollow **TpPa** structures with the pristine **TpPa** substantiates the intact chemical composition in enol form even after treatment with 1N HCl for 24 h (Fig. 2a).<sup>12</sup>

In order to assess the porosity of the as-synthesized hollow **TpPa** nanostructures, we have collected the  $\text{N}_2$  adsorption isotherms of the ZnO-nanorods, **ZnO@TpPa**, hollow **TpPa** nanostructures and pristine **TpPa** COF synthesized by solvothermal methods. As shown in Fig. 2b, the ZnO-nanorods have very low surface area ( $31\text{ m}^2\text{g}^{-1}$ ); due to the less porous architecture as a result of “oriented attachment” of ZnO-nanoparticles.<sup>11</sup> **ZnO@TpPa** shows an increase in the surface area ( $180\text{ m}^2\text{g}^{-1}$ ) due to loading of microporous **TpPa** shell on the surface of ZnO-nanorods. Further, the  $\text{N}_2$  adsorption analyses performed for hollow **TpPa** nanostructures and pristine **TpPa** COF showed typical Type-I isotherm. The surface area of **TpPa**

COF ( $479\text{ m}^2\text{g}^{-1}$ ) and hollow **TpPa** ( $447\text{ m}^2\text{g}^{-1}$ ) structures found to be almost identical (Fig. 2b). The pore size distribution plots suggest the matching pore size distribution profiles for both hollow **TpPa** structures and **TpPa** COF (Fig. S11, ESI). The increased surface area of hollow **TpPa** ( $447\text{ m}^2\text{g}^{-1}$ ) as compared to **ZnO@TpPa** ( $180\text{ m}^2\text{g}^{-1}$ ) confirms the removal of less porous ZnO-nanorods from the parent structures, leaving behind the hollow **TpPa** nanostructures composed of microporous **TpPa** COF. Although, hollow **TpPa** nanostructures have large free voids in the core, the surface area and pore size distribution remains almost identical, as these voids are very large in size (60–100 nm wide and 700–1500 nm long) for the adsorption of  $\text{N}_2$  gas molecules with a small kinetic diameter (3.64 Å) and cross sectional area ( $0.162\text{ nm}^2$ ).

The SEM and TEM analyses of the ZnO-nanorods synthesized by reported procedure showed that these ZnO-nanorods are assembled in flower shape originating from high aspect ratio nanorods of diameter of 70–130 nm and length ranging from 0.7–1.5  $\mu\text{m}$  (Section S3 and Fig. S3, ESI).<sup>11</sup> Further, the morphology of the hybrid **ZnO@TpPa** nanostructures synthesized by *in situ* loading of **TpPa** on the surface of ZnO-nanorods has been analysed by SEM and TEM analyses. **ZnO@TpPa** hybrids have adopted the same morphology of ZnO-nanorods (Fig. 3a). It is clear that these nanostructures with thick COF shells have the capsule or tube shaped morphology with the width of 200–300 nm and 750–1500 nm length adopted for individual nano-sized structures (Fig. 3b–3c). Further, these nanostructures are observed to be assembled at common centre creating the flower shaped assemblies (Fig. 3k). The close observations of these flower shaped structures at high

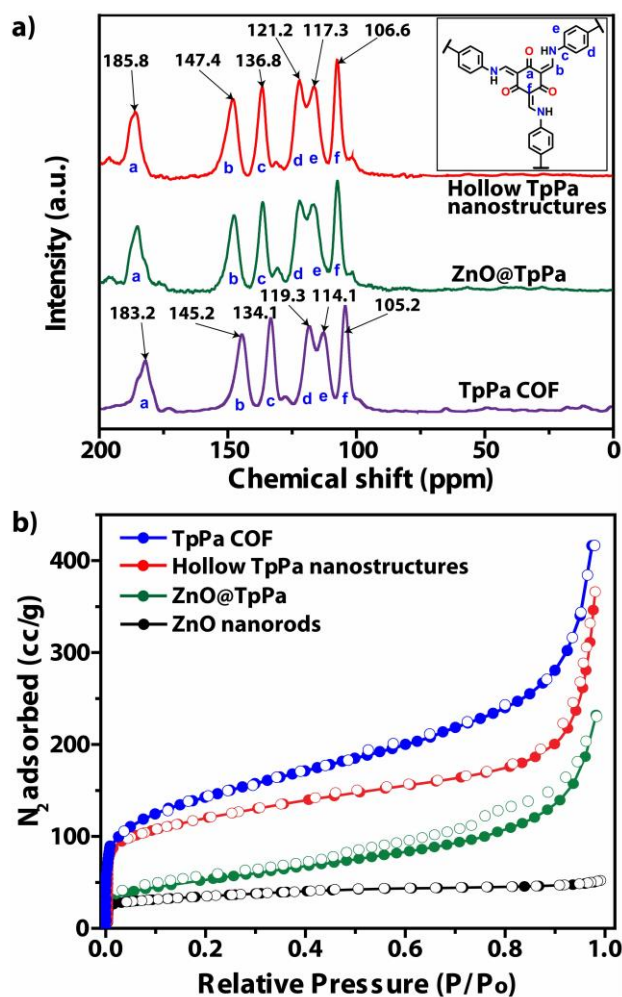


**Fig. 2** Characterization of COF nanostructures. (a) Comparison of the  $^{13}\text{C}$  CP-MAS solid-state NMR spectra of hollow **TpPa** nanostructures, **ZnO@TpPa** with the pristine **TpPa** COF. (b)  $\text{N}_2$  adsorption analyses of pristine **TpPa** COF, hollow **TpPa**, **ZnO@TpPa** and ZnO-nanorods.

resolution illustrates that these structures are composed of the individual petals, which are assembled at one end (Fig. 3c). The uniform loading of **TpPa** layer of 80–100 nm thickness on the top on ZnO-nanorods have been observed from the TEM analyses (Fig. 3d). The SAED patterns and EDAX analyses performed for the **ZnO@TpPa** have further confirmed the presence of ZnO-nanorods as core (Fig. 3d; Fig. S5–S7, ESI).

In order to achieve the hollow **TpPa** structures, the removal of ZnO core from **ZnO@TpPa** is necessary. Moreover, this spontaneous process should happen in selective manner, wherein during the core removal the morphology and chemical composition of basic shell should remain unaffected. Since, ZnO is soluble in dilute acid solution and **TpPa** COF is highly stable in 1N HCl for several days, we have treated the **ZnO@TpPa** with 1N HCl for 24 hrs in order to accomplish the selective removal of the ZnO-nanorods (Fig. 3e).<sup>12,13</sup> The samples collected after washing with water (3 X 10 ml) were analyzed by SEM and TEM analyses in order to confirm the complete removal of ZnO from **ZnO@TpPa** and determine the physical appearance of synthesized materials. The SEM and EDAX

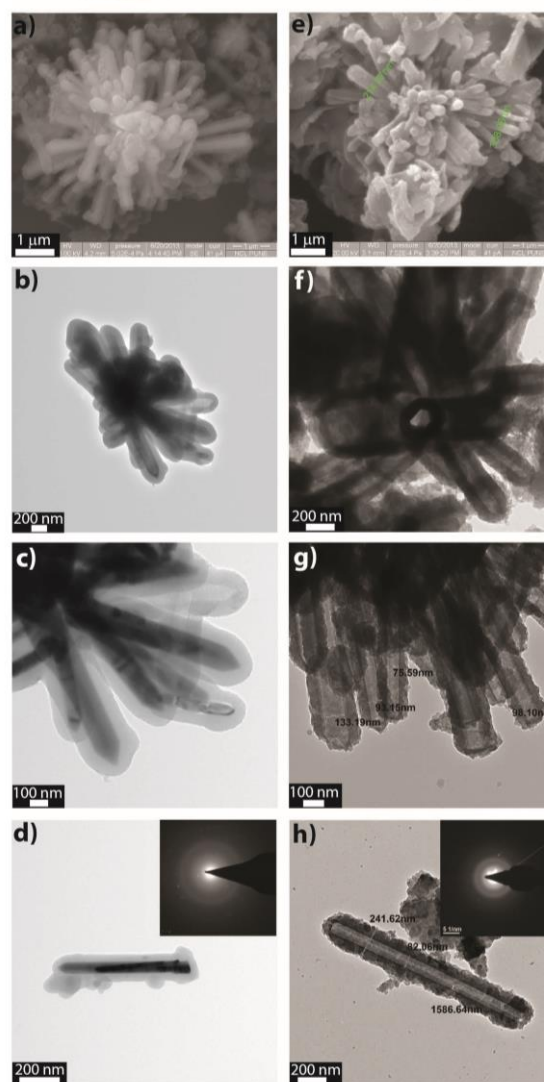
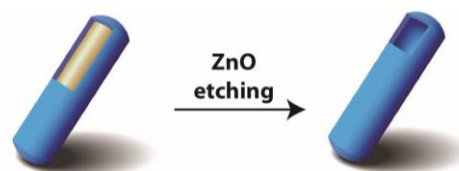


**Fig. 3** Morphological analyses of COF nanostructures. a) SEM image of ZnO-nanorods showing flower shaped morphology. b), c), d) TEM images of synthesized **ZnO@TpPa** at different resolutions showing wrapping of ZnO nanorods with **TpPa** shell (SAED pattern in Fig. 3d showing the ring pattern resembling with nano-ZnO). e) SEM image of hollow **TpPa** nanostructures after acid treatment. f), g), h) TEM images of hollow **TpPa** nanostructures obtained after acid treatment for 24 h showing formation of hollow COF structures and selective removal of ZnO with maintained morphology (SAED pattern in Fig. 3h showing absence of ring pattern).

analyses performed for hollow **TpPa** nanostructures showed the complete removal of ZnO from the core with maintained morphology (Fig. 3e; Fig. S8–S10, ESI).<sup>13</sup> As showed in Fig. 3e, the flower shaped hollow **TpPa** nanostructures with maintained shape and size were visible after the complete removal of ZnO core. Further, we have performed the TEM analyses, wherein we have observed the hollow **TpPa** structures have capsule or tube shaped

morphology similar to ZnO-nanorods and **ZnO@TpPa** (Fig. 3f–3h). Although it has been observed that in template assisted synthesis of porous polymers, during the removal of the core template from the hybrid structures, the shell collapses and decomposition of the hollow structures appears, herein we have not observed such instances due to the high stability of **TpPa** COF.<sup>12</sup> The flower shaped morphology observed for ZnO-nanorods and **ZnO@TpPa** found to be maintained in hollow **TpPa** nanostructures as well (Fig. 2f). The close observations of hollow **TpPa** structures at high resolution have confirmed that the hollow capsule shaped nanostructures are having the dimensions of 0.7–1.5  $\mu\text{m}$  in length and 200–300 nm wide (Fig. 3g). The outer walls of the hollow **TpPa** nanostructures are found to be 60–100 nm thick, whereas the inner hollow cavity measures 70–130 nm matching ideally with size of ZnO-nanorods (Fig. 3h). The inner hollow capsule shaped cavity present into **TpPa** nanostructures found to be completely free without any traces of ZnO and other impurities (Section S4 and S5, ESI).

In summary, for the first time, we have synthesized the nanometer sized hollow **TpPa** nanostructures through template-assisted replication of ZnO-nanorods. The hollow **TpPa** structures were synthesized by two step protocol, wherein first step involves the synthesis of parent **ZnO@TpPa** hybrids, which in second step after treatment with dilute acid solution yields hollow **TpPa** nanostructures, by the selective removal of ZnO-template. As synthesized hollow nanostructures composed of microporous **TpPa** shell have high surface area and these structures are highly stable in aqueous as well as acidic environment. The hollow **TpPa** structures have very large void space (60–100 nm wide and 700–1500 nm long) confined into the COF shell of 60–100 nm thickness. The nanometer sized hollow structures composed of microporous COF shell holding high stability and large scale synthesis capability might be beneficial for its imminent applications as a drug, protein and enzyme delivery materials currently being tested in our laboratory.

R.B. acknowledges CSIR's XII<sup>th</sup> Five Year Plan Project (CSC0122 and CSC0102) for funding. Financial assistance from DST (SB/S1/IC-32/2013) is acknowledged.

## Notes and references

- (a) H. C. Zeng, *J. Mater. Chem.*, 2006, **16**, 649; (b) Y. R. Ma and L. M. Qi, *J. Colloid Interface Sci.*, 2009, **335**, 1; (c) Y. Liu, J. Goebel and Y. Yin, *Chem. Soc. Rev.*, 2013, **42**, 2610.
- (a) X. W. Lou, L. A. Archer and Z. Yang, *Adv. Mater.*, 2008, **20**, 3987; (b) Z. Ren, Y. Guo, C. H. Liu, P. X. Gao, *Front Chem.*, 2013, **1**, 18; (c) K. An and T. Hyeon, *Nano Today*, 2009, **4**, 359.
- (a) F. Caruso, R. A. Caruso and H. Mohwald, *Science*, 1998, **282**, 1111. (b) Q. Zhang, W. S. Wang, J. Goebel and Y. D. Yin, *Nano Today*, 2009, **4**, 494. (c) P. Falcaro, R. Ricco, C. M. Doherty, K. Liang, A. J. Hill and M. J. Styles, *Chem. Soc. Rev.*, 2014, **43**, 5513.
- (a) A. Khanal, Y. Inoue, M. Yada and K. Nakashima, *J. Am. Chem. Soc.*, 2007, **129**, 1534; (b) Z. Wang, Y. Liu, J.-G. Jiang, M. He and Peng Wu, *J. Mater. Chem.*, 2010, **20**, 10193; (c) J. U. Park, H. J. Lee, W. Cho, C. Jo and M. Oh, *Adv. Mater.*, 2011, **23**, 3161. d) N. Kang, J. H. Park, M. Jin, N. Park, S. M. Lee, H. J. Kim, J. M. Kim and S. U. Son, *J. Am. Chem. Soc.*, 2013, **135**, 19115. e) A. Carné-Sánchez, I. Imaz, M. Cano-Sarabia and D. MasPOCH, *Nat. Chem.*, 2013, **5**, 203; (f) P. Pachfule, B. Balan, S. Kurungot and R. Banerjee, *Chem. Commun.*, 2012, **48**, 2009; (g) P. Pachfule, V. M. Dhavale, S. Kandambeth, S. Kurungot and R. Banerjee, *Chem.–Eur. J.*, 2013, **19**, 974.
- (a) P. Pàmies and A. Stoddart, *Nat. Mater.*, 2013, **12**, 957, (L. M. Arruebo, *Wiley Interdiscip. Rev.: Nanomed. Nanobiotechnol.*, 2012, **4**, 16.
- (a) J. Tamada and R. Langer, *J. Biomater. Sci. Polym. Ed.*, 1992, **3.4**, 315. b) B. Li, X. Yang, L. Xia, M. I. Majeed and B. Tan, *Sci. Rep.*, 2013, **3**, 2128; (c) X. D. He, X. W. Ge, H. R. Liu, M. Z. Wang and Z. C. Zhang, *Chem. Mater.*, 2005, **17**, 5891.
- (a) A. P. Côté, A. I. Benin, N. W. Ockwig, M. O'Keeffe, A. J. Matzger and O. M. Yaghi, *Science*, 2005, **310**, 1166; (b) J. W. Colson and W. R. Dichtel, *Nat. Chem.*, 2013, **5**, 453; (c) C. Fang, Z. Zhuang, S. Gu, R. B. Kaspar, J. Zheng, J. Wang, S. Qiu and Y. Yan, *Nat. Commun.*, 2014, **5**, 4503.
- (a) S. Chandra, S. Kandambeth, B. P. Biswal, B. Lukose, S. M. Kunjir, M. Chaudhary, R. Babarao, T. Heine and R. Banerjee, *Am. Chem. Soc.*, 2013, **135**, 17853; (b) D. B. Shinde, S. Kandambeth, P. Pachfule, R. R. Kumar and R. Banerjee, *Chem. Commun.*, 2015, **51**, 310; (c) A. Thomas, *Angew. Chem. Int. Ed.*, 2010, **49**, 8328; (d) X. Feng, X. Ding and D. Jiang, *Chem. Soc. Rev.*, 2012, **41**, 6010.
- (a) S. Kandambeth, V. Venkatesh, D. B. Shinde, S. Kumari, A. Halder, S. Verma and R. Banerjee, *Nat. Commun.*, 2015, **6**, DOI:10.1038/ncomms7786. (b) J. Jin, B. Kim, N. Park, S. Kang, J. H. Park, S. M. Lee, H. J. Kim and S. U. Son, *Chem. Commun.*, 2014, **50**, 14885.
- S. Kandambeth, A. Mallick, B. Lukose, M. V. Mane, T. Heine and R. Banerjee, *J. Am. Chem. Soc.*, 2012, **134**, 19524.
- B. Liu and H. C. Zeng, *J. Am. Chem. Soc.*, 2003, **125**, 4430.
- The high stability of **TpPa** COF which has been synthesized via combined reversible and an irreversible organic reaction in aqueous, acid and base mediums arises from the irreversible nature of the enol-to-keto tautomerism acquired during the COF synthesis.
- The attempts to remove the ZnO-nanorods from **ZnO@TpPa** to generate hollow **TpPa** nanostructures in less than 24 h time interval were unsuccessful, as the TEM and EDAX analyses performed for the samples treated with 1N HCl for 18 h have showed the presence of ZnO-nanorods to some extent (Section S6, ESI).